Potential dependent adsorption of anthraquinone-2,7-disulfonate on mercury†

Joseph P. O'Kelly and Robert J. Forster*

School of Chemical Sciences, Dublin City University, Dublin 9, Ireland

Received 27th May 1998, Accepted 7th September 1998

Monolayers of anthraquinone-2,7-disulfonic acid, 2,7-AQDS, have been formed by equilibrium adsorption onto mercury electrodes. In low pH electrolytes, cyclic voltammetry is nearly ideal with a peak-to-peak splitting of 8 ± 2 mV, and a full width at half maximum of 57 ± 1 mV, being observed for scan rates less than 3 V s^{-1}. The dependence of the surface coverage of 2,7-AQDS as measured using voltammetry on its bulk concentration is described by the Langmuir isotherm over the concentration range 0.06–9 μM. A saturation surface coverage, Γ_s, of $(8.7 \pm 0.5) \times 10^{-11}$ mol cm^{-2} and an adsorption coefficient, β, of $(5.6 \pm 0.5) \times 10^5$ M^{-1} are observed where the supporting electrolyte is 1.0 M $HClO_4$. Consistent with the formation of an organic film, the double layer capacitance, C_{dl}, as measured at −0.700 V, decreases from approximately 40 μF cm^{-2} in the absence of dissolved 2,7-AQDS to 10 μF cm^{-2} when the bulk concentration exceeds 10 μM. By measuring the potential dependence of C_{dl} as the bulk concentration of 2,7-AQDS is varied systematically, an insight into the potential dependence of the free energy of adsorption, $\Delta G^{\ddagger}_{ads}$, has been obtained. These data reveal that $\Delta G^{\ddagger}_{ads}$ is similar for both fully oxidised and fully reduced monolayers. However, these quinonoid monolayers are least strongly bound ($\Delta G^{\ddagger}_{ads} = -28.5$ kJ mol^{-1}) when the film exists in the quinhydrone form.

Introduction

Depositing monomolecular films using self-assembly or spontaneous adsorption represents an important approach to controlling the properties of the electrode/solution interface.[1–5] While numerous investigations have focused on the physical and chemical properties of these monolayers,[6–8] much less is known about the kinetics and thermodynamics of adsorption in systems of this type. Molecular adsorption onto metal electrodes is known to be profoundly influenced by the specific properties of the substrate and by the state of charge of the surface.[9] In particular, the applied potential plays an important role in determining the stability and configuration of adsorbates.[10,11] For redox active monolayers, the applied potential may influence the adsorption process, not only by changing metal–adsorbate interactions, but also by changing adsorbate–adsorbate interactions through changes in the redox composition of the film.[12]

In recent years, there has been a stronger focus on using Faradaic rather than capacitance measurements to probe these issues. This situation is somewhat surprising given the sensitivity of the interfacial capacitance to the presence of adsorbates. One of the difficulties associated with obtaining accurate capacitance data on redox active films is the difficulty in separating Faradaic and capacitive currents when making measurements close to the formal potential. However, we have demonstrated that by using high speed chronoamperometry, it is possible to efficiently time resolve, and therefore separate, these current contributions under a wide range of experimental conditions.[13,14] In this contribution, we apply this approach to studying the effect of potential on the formation of anthraquinone-2,7-disulfonic acid (2,7-AQDS) monolayers.

The potential dependence of the differential capacitance of metal electrodes can exhibit well defined maxima at certain voltages in the presence of physically adsorbed neutral molecules.[15] These peaks are interpreted as evidence of adsorption/desorption at the electrode surface. However, the capacitance behaviour of organic monolayers that are chemisorbed to the electrode surface is quite different and adsorption/desorption peaks are absent because a more or less permanent film is formed.[16] We are interested in measuring the interfacial capacitance to diagnose the strength of 2,7-AQDS adsorption over a wide range of potentials encompassing regions where the film is electroactive and regions far from the formal potential of the quinone/hydroquinone redox reaction.

The ability to time-resolve capacitive and Faradaic currents makes it possible to probe the potential dependence of the interfacial capacitance as the bulk concentration, and hence surface coverage, of a surface active molecule is systematically varied. In this way, we have obtained a useful insight into the potential dependent adsorption of electroactive species that are reversibly adsorbed onto electrode surfaces.

Experimental

Materials and procedures

The disodium salt of anthraquinone-2,7-disulfonic acid (2,7-AQDS) was obtained from BASF (Ludwigshafen, Germany). All electrolytes were prepared using Milli-Q purified water. Spontaneously adsorbed monolayers were formed by immersing the electrodes in the supporting electrolyte solution containing the anthraquinone at the desired concentration, typically in the low μM range. Since adsorption is reversible in this system, subsequent experiments were carried out with this concentration of 2,7-AQDS present in solution. The highest concentration of anthraquinone in solution was 10 μM. To ensure that the current observed is dominated by the redox reactions of the monolayer rather than the solution phase anthraquinone, experiments designed to probe the concentration dependence of the surface coverage were performed at relatively short timescales. For example, for the dropping mercury electrode used in this study, for scan rates greater than 10 V s^{-1} the maximum contribution from diffusion to the voltammetric peak current is less than 2% even in 10 μM

† Presented at EIRELEC '98, Howth, Co. Dublin, Ireland, March 26–28, 1998.

2,7-AQDS solutions.[9] All measurements were undertaken when the surface coverage had reached equilibrium with the bulk concentration of 2,7-AQDS, *i.e.*, when repeated voltammetric cycling revealed an unchanging peak current.

Apparatus

All measurements were performed using conventional three-electrode electrochemical cells thermostated to 25 ± 0.2 °C using a Julabo F10-HC (Kutztown, PA, USA) refrigerated circulating bath. The electrolytic solutions were degassed using nitrogen and a blanket of nitrogen was maintained over the solution during all experiments. All potentials are quoted with respect to a BAS (West Lafayette, IN, USA) Ag/AgCl gel-filled reference electrode. Cyclic voltammetry was performed using a PAR EG&G Model 273 (Wokingham, UK) potentiostat/galvanostat interfaced to a PAR EG&G model 270 mercury electrode. Chronoamperometry was carried out using a CH Instruments (Memphis, TN, USA) Model 660 Electrochemical Workstation. The area of the mercury electrode was determined by recording cyclic voltammograms of 1,4-benzoquinone under radial and semi-infinite linear diffusion conditions.[17] Using the values obtained for the limiting and peak currents, an electrode area of 0.017 ± 0 0.002 cm^2 was obtained. This value agrees with that obtained by dispensing, and then subsequently drying and weighing, one hundred mercury drops.

Results and discussion

General electrochemical properties

Fig. 1 shows representative cyclic voltammograms for a mercury electrode immersed in a 5 μM solution of 2,7-AQDS in 1.0 M $HClO_4$. The peak shapes are independent of scan rate up to at least 20 V s^{-1} and the peak height varies linearly with sweep rate, v, rather than the $v^{1/2}$ dependence expected for a freely diffusing species.[9] These voltammograms are consistent with those expected for an electrochemically reversible reaction involving a surface confined redox-active species.[18,19] Therefore, consistent with previous reports on structurally related anthraquinones[20,21] it appears that 2,7-AQDS adsorbs onto the surface of the mercury electrode to give an electroactive film.

For a surface confined species in which there are no interactions between adsorbates, and an equilibrium is rapidly established between the applied potential and the redox

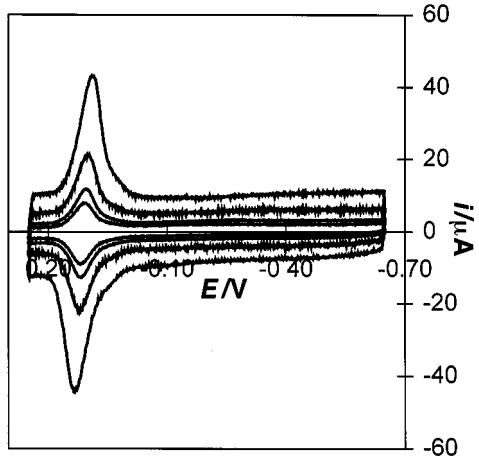

Fig. 1 Cyclic voltammograms for a mercury electrode immersed in a 5 μM solution of 2,7-AQDS in 1.0 M $HClO_4$. Scan rates from top to bottom are 20, 10, 5, and 3 V s^{-1}. Cathodic currents are up and anodic currents are down. The initial potential is −0.650 V and the electrode area is 0.017 cm^2.

composition of the film, a zero peak-to-peak splitting and a full width at half maximum (FWHM) of 90.6/n, where n is the number of electrons transferred, are expected.[9] We typically observe a peak-to-peak splitting and an FWHM of 8 ± 2 and 57 ± 1 mV, respectively, at scan rates slower than 3 V s^{-1} in 1 M $HClO_4$. The magnitude of the FWHM suggests that this redox reaction involves the transfer of two electrons, at least in low pH electrolytes. This result is consistent with our previous work[13,14,21–23] which revealed that in acidic solutions reduction of anthraquinone monolayers proceeds by a two-proton, two-electron transfer mechanism.

When the time constants of the voltammetric experiment and electron transfer are comparable, one expects the rate of electron transfer across the metal/film interface to influence the voltammetric response.[9] A shift in both the anodic and cathodic peak potentials, that cannot be attributed to iR drop, and a non unity slope magnitude in a plot of the peak current, i_p, *versus* the scan rate are evidence that the electrode kinetics influence the overall response. That the experimental i_p increases linearly with increasing v up to 20 V s^{-1} with an absolute slope of near unity (|slope| = 0.98 ± 0.06) indicates that for scan rates up to 20 V s^{-1} the experimental timescale is longer than that for electron transfer. For scan rates above 20 V s^{-1}, the slope observed in a plot of i_p *versus* v decreases significantly, and the current tends to become independent of the scan rate for values greater than approximately 200 V s^{-1}. Given that the time constant for a cyclic voltammetry experiment in which the scan rate is 20 V s^{-1} is approximately 1 ms, these observations suggest that the standard electron transfer rate constant, $k°$, is at least 800 s^{-1}. That electron and proton transfer are coupled in these systems, and that the heterogeneous kinetics are not adequately described by simple Butler–Volmer kinetics, complicates fitting of the data to, for example Laviron's model,[18] to extract accurate heterogeneous rate constants.

For potentials far from $E°'$, the voltammetric response is dominated by the double layer charging current, i_c. The charging current observed in the absence of dissolved 2,7-AQDS is at least twice as large as that observed when its bulk concentration is 10 μM. Therefore, that the charging current observed in Fig. 1 is independent of the applied potential between approximately 0.00 and −0.65 V suggests that the anthraquinone moieties remain adsorbed over the entire potential range investigated and desorb only at potentials negative of −0.65 V.[16] That the peak shapes do not change significantly when cycled repeatedly at temperatures up to 40 °C, over at least 30 min, indicates that adsorbed films of 2,7-AQDS are both electrochemically and thermally stable.

The pH dependence of cyclic voltammograms for surface confined 2,7-AQDS in unbuffered electrolyte is shown in Fig. 2. As discussed above, at a pH of 1.5 the voltammetric response of monolayers of 2,7-AQDS is centred at 0.00 V and is unusually ideal. As the pH of the contacting electrolyte is increased, the voltammetric wave initially shifts in a negative potential direction but becomes independent of the solution pH above pH 4.1. In the very narrow pH range 3.9 to 4.1 two two-electron waves are observed. The sum of the charges under these two peaks, 390 ± 5 nC, is identical to that found under either of the two-electron peaks observed at high or low pH. This observation suggests that over the entire pH range investigated, the redox reactions involve the transfer of two electrons but for 3.9 ≤ pH ≤ 4.1, two chemically distinct species co-exist on the electrode surface.

Adsorption isotherms

The total charge, Q, introduced or withdrawn to reduce or oxidise the immobilised species, can be found from the area under the voltammetric peak after correcting for the background

charging current.[9] This charge, together with the area of the electrode, A, is used to calculate the surface coverage, Γ:

$$\Gamma = \frac{Q}{nFA} \quad (1)$$

where n is the number of electrons transferred, F is Faraday's constant and A is the electrode area.

The surface coverage can be used to determine the area occupied by individual adsorbates which may provide an insight into the orientation of the compound on the electrode, *i.e.*, flat or edge-on.[24] Molecular orientation has important implications in the chemistry of adsorbed compounds, *e.g.*, the oxidation pathway for adsorbed aromatics on Pt is known to depend on their orientation.[25] The saturation surface coverage, Γ_s, as measured using cyclic voltammetry in an electrolytic solution containing a relatively high concentration of 2,7-AQDS (10 μM) was $(7.2 \pm 0.6) \times 10^{-11}$ mol cm^{-2}. This surface coverage gives an area of occupation per molecule of 230 ± 012 Å^2. This area is consistent with that reported by Faulkner and co-workers[20] (200 ± 10 Å^2) for 2,6-AQDS suggesting that the substitution pattern of the anthraquinone does not significantly affect the packing density. It is perhaps important to note that Soriaga and Hubbard[26] observed a limiting coverage of 131 ± 7 Å^2 for 2,6-AQDS adsorbed on platinum indicating that the nature of the electrode material influences the monolayer structure significantly.

In order to define the adsorption isotherm, the surface coverage of 2,7-AQDS at equilibrium was determined using the area under the voltammetric peak, after correcting for the contribution from double layer charging, as the solution concentration of the anthraquinone moiety was systematically varied. Fig. 3 shows the change in surface coverage as the solution concentration of 2,7-AQDS is varied from 5.5×10^{-8} to 9.0×10^{-6} M. These data show that the surface coverage does not increase beyond the plateau value even if the bulk concentration of 2,7-AQDS is increased significantly. This result indicates that this system tends to form monolayers rather than multilayers. Moreover, that Γ is essentially independent of the bulk 2,7-AQDS concentration for $10\ \mu M \leq C_b \leq 1\ 0$ mM suggests that concentration induced molecular reorientation does not occur in this system unlike the situation frequently found for quinones on platinum.[27]

The Langmuir isotherm[9,28] describes equilibrium adsorption for the situation where lateral interactions between the adsorbed molecules are absent or are independent of the surface coverage, the electrode surface is homogeneous, and the limiting surface coverage is dictated simply by the size of the adsorbate. That the voltammetric response illustrated in Fig. 1 is nearly ideal, and that both adsorption and desorption of the anthraquinone occurs rapidly and reversibly, suggests that the Langmuir isotherm may be an appropriate description of adsorption in this case. This isotherm is described by the following expression:

$$\frac{\Gamma_s}{\Gamma_s - \Gamma_i} = \beta_i C_i \quad (2)$$

where β_i and C_i are the adsorption coefficient and the solution phase concentration of species i, respectively. In the following discussions, activity coefficients are incorporated into the adsorption coefficient. The line in Fig. 3 is the best fit Langmuir isotherm. That satisfactory agreement between experiment and theory is obtained suggests that this model may provide an appropriate description of the experimental data.

The Langmuir isotherm predicts that a plot of C_i/Γ_i *vs.* C_i should be linear, and that the saturation surface coverage, Γ_s, and the adsorption coefficient, β_i, can be obtained from the slope and intercept, respectively:

$$\frac{C_i}{\Gamma_i} = \frac{1}{\Gamma_s} C_i + \frac{1}{\Gamma_s} \beta_i \quad (3)$$

The inset of Fig. 3 shows that a plot of this type is satisfactorily linear ($R^2 = 0.98$) and the slope yields an estimate of $(9.0 \pm 0.5) \times 10^{-11}$ mol cm^{-2} for the saturation surface coverage, Γ_s. The adsorption coefficient, β_i, which describes the strength of adsorption, is $(5.2 \pm 0.5) \times 10^5$ M^{-1}. Significantly, the adsorption coefficient for the system investigated here is an order of magnitude smaller than that found for 2,6-AQDS [$(5.2 \pm 0.7) \times 10^6$ M^{-1}].[20] This observation suggests that while the location of the sulfonate groups does not significantly affect the monolayer coverage (*vide supra*) it may be an important factor in determining the strength of adsorption. The adsorption coefficient can be used to calculate the free energy of adsorption, $\Delta G^{\ddagger}_{ads}$:

$$-\Delta G^{\ddagger}_{ads} = RT \ln \beta_i \quad (4)$$

which includes contributions from concentration independent adsorbate–adsorbate and potential dependent adsorbate-electrode interactions. The free energy of adsorption at $E^{\circ\prime}$ is −32.8 ± 0.3 kJ mol^{-1}.

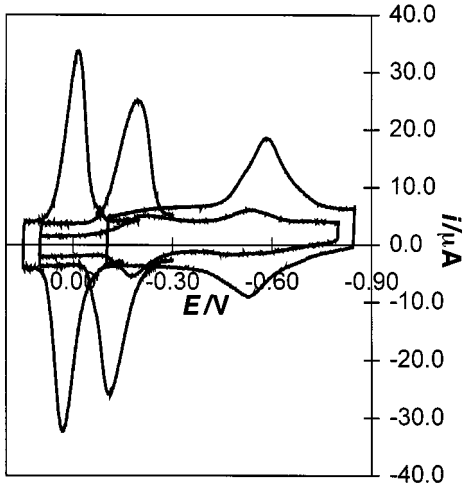

Fig. 2 Cyclic voltammograms for a 0.017 cm^2 mercury electrode immersed in a 5 μM solution of 2,7-AQDS as the pH of the unbuffered contacting electrolyte solution is, from left to right, 1.1, 3.8, 1 (double peak) and 5.1. The scan rate is 10 V s^{-1} and the supporting electrolyte is 0.10 M $LiClO_4$. Cathodic currents are up and anodic currents are down. The initial potential is −0.650 V.

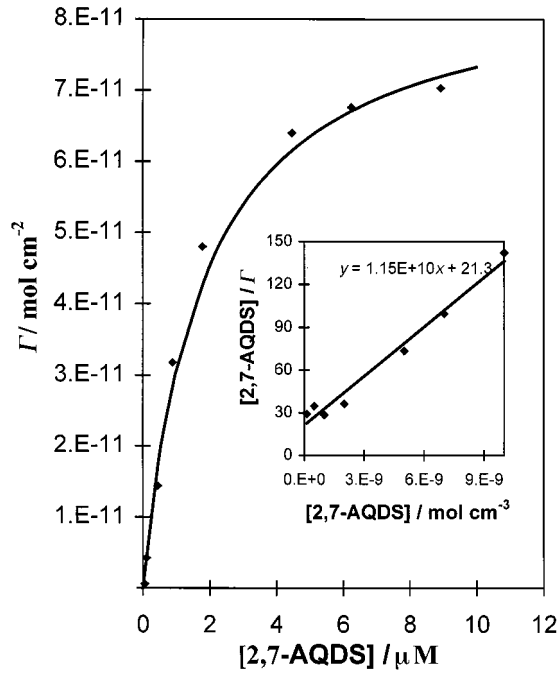

Fig. 3 Relationship between surface coverage and bulk concentration of 2,7-AQDS. The solid line is the best fit to the Langmuir isotherm. The inset illustrates data plotted according to the linearised Langmuir isotherm. The supporting electrolyte is 1.0 M $HClO_4$.

Potential dependence of adsorption strength

Voltammetry can provide a powerful insight into the effect of the applied potential on the surface coverage and strength of adsorption when a molecule adsorbs *irreversibly* onto an electrode surface.[12,29] This understanding can be achieved because the applied potential can be controlled during monolayer deposition and the surface coverage can be measured in a blank electrolyte solution that does not contain any of the adsorbate of interest. This approach is not useful when adsorption is *reversible* since transferring the coated electrode into blank electrolyte would change the equilibrium surface coverage. However, the double layer capacitance, C_{dl}, is sensitive to the nature and extent of surface modification and its potential dependence can be measured in the presence of the dissolved anthraquinone.[14,22] Therefore, we have used potential step chronoamperometry to investigate how the double layer capacitance, C_{dl}, depends on the applied potential as the concentration of 2,7-AQDS in solution is systematically varied. While recognising that chronoamperometry is not an especially sensitive technique for measuring the interfacial capacitance, it has the advantage that double layer charging and Faradaic currents can be time-resolved[13] and the technique is easily implemented.

Chronoamperometry

In these experiments, the potential was stepped from an initial value E_i using a pulse amplitude of 30 mV and the resulting current response was recorded. Between successive measurements, E_i was increased by 30 mV from −0.700 to +0.100 V. The charging current, i_c, decays exponentially in time according to eqn. (5):[30]

$$i_c(t) = (\Delta E/R) \exp(-t/RC_{dl}) \quad (5)$$

where ΔE is the pulse amplitude and R is the total cell resistance.

Eqn. (5) predicts that when the potential is stepped in a region where the redox composition of the monolayer does not change, *i.e.*, far from $E^{\circ\prime}$, a plot of the logarithm of the current observed *vs.* time should be linear. When the potential is stepped in a region close to $E^{\circ\prime}$, the current response at short times is dominated by double layer charging with Faradaic current due to oxidation of the adsorbed 2,7-AQDS moieties occurring at longer times.[13,14] Therefore, a plot of the logarithm of the short timescale current *vs.* time should be linear. Fig. 4 shows how semi-log plots depend on the applied potential for monolayer modified mercury electrodes. The resistance and double layer capacitance were determined from the intercepts and slopes of these lines, respectively, and the data are presented in Table 1.

Fig. 4 reveals that the intercepts of semi-log plots are independent of the applied potential. Moreover, Table 2 shows that the resistance changes by less than 25% as the composition of the electrolyte solution is systematically varied from one that does not contain any dissolved 2,7-AQDS to one where the anthraquinone concentration is 10 μM. That R is relatively independent of both the applied potential and the anthraquinone concentration suggests that the solution resistance dominates the total cell resistance and that the film resistance makes only a minor contribution.

Interfacial capacitance

For an electrode coated with a modifying film, both the diffuse layer capacitance from solution, C_{dif}, and the film capacitance, C_{film}, may contribute to the overall double layer capacitance:[16,31]

$$\frac{1}{C_{dl}} = \frac{1}{C_{film}} + \frac{1}{C_{dif}} \quad (6)$$

Only the diffuse layer capacitance depends on the applied potential and the concentration of supporting electrolyte[9] and the effect of monolayer assembly on the interfacial potential distribution can be diagnosed by measuring C_{dl} as both the applied potential and the bulk concentration of 2,7-AQDS are systematically varied.

The slopes of the best fit lines to the semi-log plots of Fig. 4 depend on the applied potential indicating that the double layer capacitance is potential dependent. Fig. 5 illustrates the potential dependence of the interfacial capacitance as the bulk concentration of 2,7-AQDS is systematically varied. This figure shows that strikingly different voltage dependences are

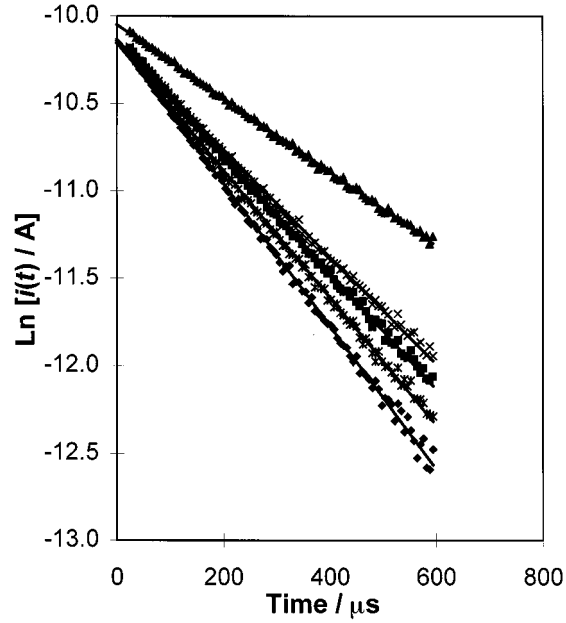

Fig. 4 Effect of the applied potential on plots of the logarithm of the capacitive current *vs.* time for mercury electrodes modified with dense monolayers of 2,7-AQDS.

Table 1 Effect of potential on the total cell resistance and interfacial capacitance observed for a mercury electrode modified with a close packed monolayer of 2,7-AQDS

Potential/V	Resistance[a]/Ω	Capacitance[a]/μF cm^{-2}
−0.220	760(35)	11.6(0.9)
−0.340	750(20)	13.1(1.0)
−0.430	700(25)	15.8(1.1)
−0.520	770(20)	14.7(0.8)
−0.670	770(28)	12.6(0.9)

[a] Resistance and capacitance values quoted are the average of at least three independent chronoamperometric experiments on separate monolayers. The errors are quoted in parentheses.

Table 2 Effect of 2,7-AQDS concentration on the total cell resistance and interfacial capacitance as measured at −0.430 V

[2,7-AQDS]	Resistance[a]/Ω	Capacitance[a]/μF cm^{-2}
0	684(38)	33.1(1.8)
1	756(43)	27.8(1.4)
2	766(51)	25.8(2.1)
7	803(39)	17.2(1.3)
10	890(55)	15.8(0.8)

[a] Resistance and capacitance values quoted are the average of at least three independent chronoamperometric experiments on separate monolayers. The errors are quoted in parentheses.

observed for the monolayer modified electrodes compared to the pristine metal surfaces. In particular, the double layer capacitance is measurably smaller for the coated electrode than for an unmodified interface over the entire potential range investigated, *e.g.*, at the formal potential, the capacitance decreases from 31 μF cm^{-2} for the bare electrode to 17 μF cm^{-2} for a 10 μM solution, and only the clean mercury surfaces show a pronounced minimum. The reduced capacitance in the presence of 2,7-AQDS is consistent with the cyclic voltammetry data presented earlier which indicated that the surface coverage increases from approximately half of a close packed monolayer to approximately full monolayer coverage as the bulk concentration of the anthraquinone is increased from 2 to 10 μM. The data illustrated in this figure are highly reproducible and no detectable hysteresis was observed between successive potential scans, or if the direction of scanning was reversed. These observations suggest that either the structure of the film is static or that it rapidly equilibrates with the applied potential.

A minimum in C_{dl} is expected at the potential of zero charge (p.z.c.) which represents the potential at which there is no excess charge on either the electrode or solution sides of the interface.[9] Fig. 5 reveals that for the clean mercury interface a minimum in the capacitance occurs at −415 ± 15 mV. This value of the p.z.c. is consistent with that expected for a mercury electrode in contact with a dilute, non-surface active electrolyte.[9]

The pK_as of the hydroquinone groups within the reduced form of the adsorbate are 7.7 and 10.5.[32,33] However, the pK_as for the oxidised or quinone form of the monolayer are approximately 6 pH units lower. Therefore, given that the sulfonic acid groups are deprotonated at the pH of this study (5.5), the reduced monolayer is electrostatically neutral while the oxidised form has a charge of 2−. Under these circumstances, one would expect the potential of zero charge for the monolayer to depend on its redox composition. However, it is not possible to identify the p.z.c. for the anthraquinone derivatised electrodes since, even in the presence of 2,7-AQDS concentrations as low as 2 μM, no well-defined minimum in the interfacial capacitance is observed over the potential range investigated. We note that the formal potential in 0.05 M NaF is −415 mV, *i.e.*, the p.z.c. observed for the bare electrode, and $E^{\circ\prime}$ for the monolayer, are coincident, making it difficult to determine the effect of monolayer formation on the p.z.c.

Fig. 5 shows that a distinct maximum in C_{dl} is observed at approximately −415 mV. That a distinctive peak is observed suggests that this behaviour is not due to imperfections within the anthraquinone monolayer or voltage dependent penetration of water or ionic species into the film. An alternative explanation is that the surface coverage is lower at this potential. To investigate this possibility, we have probed how the interfacial capacitance depends on the bulk concentration, and hence surface coverage, of 2,7-AQDS. The dependence of the interfacial capacitance on the surface coverage can be described using the parallel capacitor model originally proposed by Delahay.[34] In this model, the double layer capacitance for incomplete monolayers is represented by an equivalent circuit composed of two capacitors in parallel representing the contributions from the bare and modified fractions of the electrode surface:

$$C_{dl} = C_{mono} + (C_{bare} - C_{mono})(1 - \theta) \quad (7)$$

where C_{bare} and C_{mono} are the capacitances of the bare and densely coated electrodes respectively, and θ is the fractional surface coverage. Fig. 6 illustrates how the interfacial capacitance, as measured at the formal potential, changes as the bulk concentration is systematically varied from 1 to 10 μM. The capacitance decreases from 31 μF cm^{-2} for the bare electrode to 17 μF cm^{-2} when the concentration in solution is 10 μM. Fig. 3 demonstrated that the Langmuir isotherm provides an adequate description of the dependence of the surface coverage of 2,7-AQDS on its bulk concentration. We have combined Delahay's parallel capacitor model with the Langmuir isotherm to allow the potential dependence of Γ to be probed through measurements of C_{dl}. Eqn. 8 summarises this model:[14]

$$\frac{[2,7\text{-AQDS}]}{(C_{bare} - C_{dl})} = \frac{1}{C_{mono}}[2,7\text{-AQDS}] + \frac{1}{C_{mono}\beta_i} \quad (8)$$

where [2,7-AQDS] represents the solution concentration of 2,7-AQDS. According to eqn. (8), the slope and intercept obtained from a plot of [2,7-AQDS]/(C_{bare} − C_{dl}) *vs.* [2,7-AQDS] can be used to determine the capacitance corresponding to a close packed monolayer and the adsorption coefficient, respectively. The inset of Fig. 6 illustrates a plot of this type using values of C_{dl} measured at $E^{\circ\prime}$. This plot is linear (R^2 = 0.9936) suggesting that the parallel capacitor model provides an accurate description of adsorption for 2,7-AQDS films. The slope of the inset in Fig. 6 reveals a capacitance for a dense monolayer, C_{mono}, of 22 μF cm^{-2} which compares

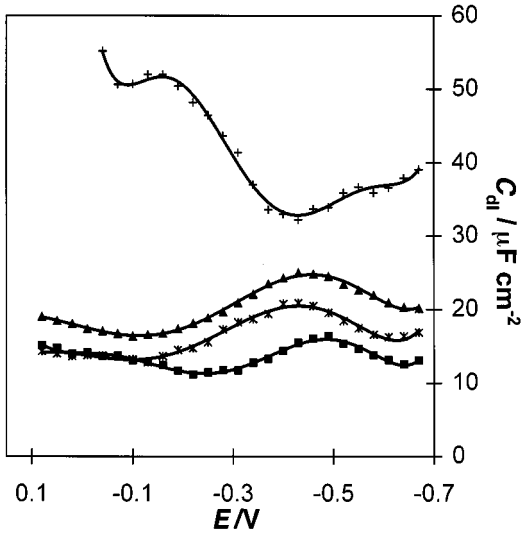

Fig. 5 Double layer capacitance as a function of applied potential as the concentration of 2,7-AQDS in solution is systematically varied. The curves, from top to bottom, represent the capacitance of electrodes immersed in 0.05 M NaF containing 0, 2, 5, and 10 μM 2,7-AQDS. Typical error bars are less than 2 μF cm^{-2}.

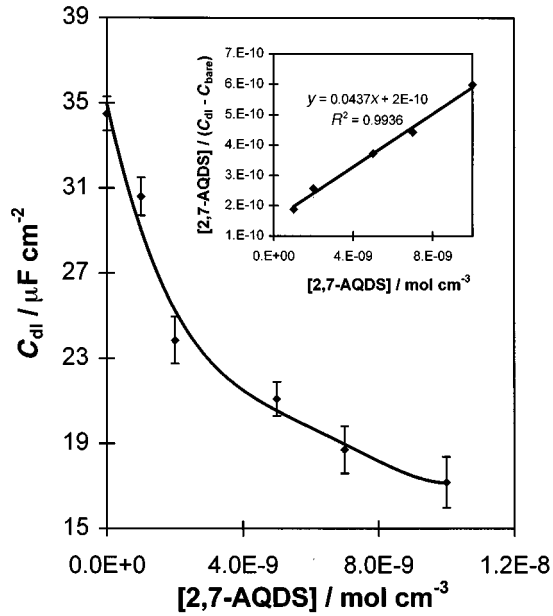

Fig. 6 Dependence of the double layer capacitance as measured at the formal potential on the bulk concentration of 2,7-AQDS. The inset illustrates data linearised according to a parallel capacitor model. The supporting electrolyte is 0.05 M NaF.

favourably with the value of 17 μF cm^{-2} obtained directly from chronoamperometry where the bulk concentration of 2,7-AQDS is 10 μM. The adsorption coefficient of (2.2 ± 0.5) × 10^5 M^{-1} obtained from the intercept of this plot is in reasonable agreement with the value of (5.6 ± 0.5) × 10^5 M^{-1} obtained from the linearised Langmuir isotherm (Fig. 3). That the capacitance and voltammetric results agree, indicates that measurements of C_{dl} can be used to probe the strength of adsorption in this system, at least at E°′.

Fig. 7 shows data obtained at potentials away from $E^{\circ\prime}$ and reveals that plots of [2,7-AQDS/($C_{bare} - C_{dl}$) *vs.* [2,7-AQDS] are linear at all potentials investigated. This linearity suggests that the parallel capacitor model provides a meaningful insight into the potential dependence of both C_{mono} and β.

Free energy of adsorption

That adsorption in this system is described by the Langmuir adsorption isotherm suggests that adsorbate–adsorbate interactions are either absent or do not depend strongly on the redox composition or packing density of the monolayer. However, it is possible that adsorbate–electrode interactions depend on the applied potential, thus making the free energy of adsorption, $\Delta G^{\ddagger}_{ads}$, potential dependent. The intercepts of the plots shown in Fig. 7 have been used in conjunction with eqn. (4) and (8) to determine the potential dependence of the free energy of adsorption and the data are illustrated in Fig. 8. At potentials far from $E^{\circ\prime}$, where only the oxidised or reduced form of the monolayer exist, the free energy of adsorption is large, but is insensitive to the applied potential. For example, $\Delta G^{\ddagger}_{ads}$ differs by only 1.5 kJ mol^{-1} when measured at −0.21 or −0.67 V, where the monolayer is fully oxidised and reduced, respectively. This observation suggests that $\Delta G^{\ddagger}_{ads}$ is relatively insensitive to the applied potential provided that only a single redox form exists on the electrode surface.

The most striking feature of Fig. 8 is that the absolute value of $\Delta G^{\ddagger}_{ads}$ reaches a minimum at approximately −415 mV, *i.e.*, the adsorbates are least strongly bound at this potential. This potential corresponds to both the p.z.c. of the bare mercury surface and the formal potential of the quinone/hydroquinone redox reaction. Unlike potentials that are significantly positive or negative of the formal potential, at $E^{\circ\prime}$ the monolayer may contain three distinct redox forms of the adsorbate, namely the quinone, hydroquinone and semiquinone forms. Capacitance data do not allow us to discriminate between these different redox states preventing a complete interpretation of the available data. However, a minimum in $\Delta G^{\ddagger}_{ads}$ at the p.z.c. is not expected since the oxidised form of the adsorbate has a 2− charge due to dissociation of the two sulfonic acid groups. Under these circumstances, one would anticipate a larger $\Delta G^{\ddagger}_{ads}$ at potentials positive of the p.z.c. While future papers will report results at other pHs where the p.z.c. and $E^{\circ\prime}$ are not co-incident, it is likely that the interactions between the electrode and the co-adsorbed quinones, hydroquinones and perhaps semiquinones that exist at $E^{\circ\prime}$, as well as, acid/base reactions influence the observed response.

Conclusions

The electrochemistry of anthraquinone-2,7-disulfonate monolayers has been investigated and found to be unusually ideal under conditions of low electrolyte pH. In particular, the effects of adsorbate concentration and the applied potential on the adsorption strength have been probed. The dependence of the surface coverage on the bulk concentration of 2,7-AQDS is adequately described by the Langmuir adsorption isotherm. The area occupied per molecule suggests that the adsorbate binds to the surface of the electrode in a flat orientation and that reorientation does not occur, at least not for bulk anthraquinone concentrations up to 10 μM. This resistance to reorientation most likely arises because of entropy considerations. In the flat orientation, each of the three fused rings can interact with the mercury surface, whereas a perpendicular adsorbate would permit only limited anthraquinone–electrode interaction but more extensive lateral interactions through π-stacking.

The double layer capacitance, C_{dl}, has been probed as a function of the applied potential and the solution concentration of 2,7-AQDS. While C_{dl} depends strongly on the concentration of 2,7-AQDS it appears to be only weakly dependent on the applied potential. The concentration dependence of C_{dl} is described by a parallel capacitor model which has been used to probe the potential dependence of the free energy of adsorption. The potential dependence of the free energy of adsorption

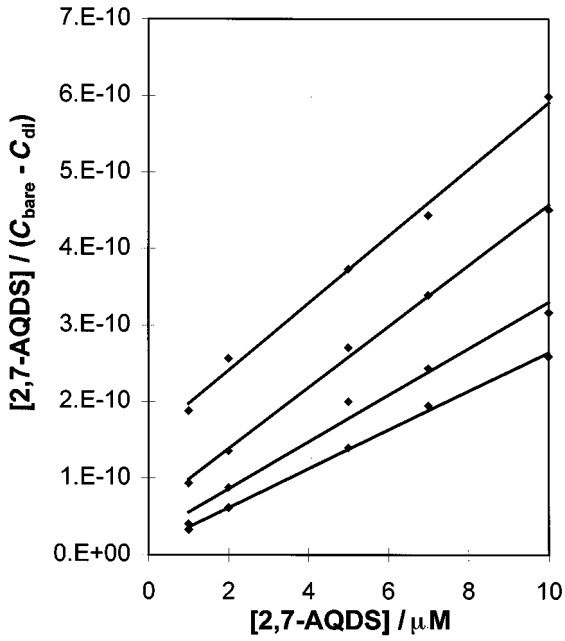

Fig. 7 Potential dependence of capacitance data linearised according to the parallel capacitor model. From top to bottom, the potentials are, −0.460, −0.520, −0.310 and −0.190 V, respectively. The supporting electrolyte is 0.05 M NaF.

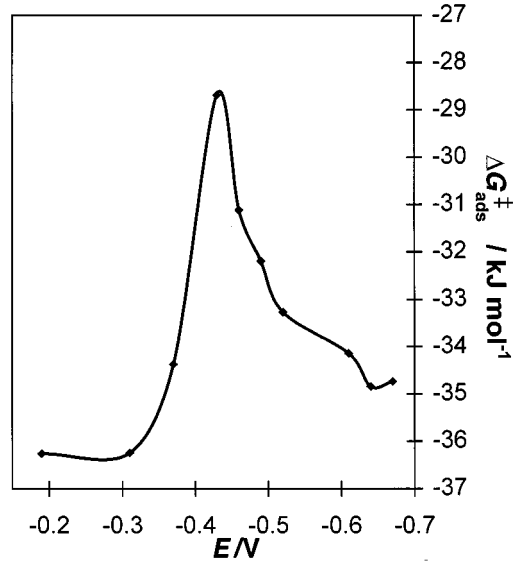

Fig. 8 Dependence of the free energy of adsorption on the applied potential. The supporting electrolyte is 0.05 M NaF.

indicates that the monolayer is least strongly bound at −415 ± 15 mV which coincides with the formal potential of 2,7-AQDS in 0.05 M NaF and the p.z.c. of the unmodified mercury interface. We have found that the ionic strength of the supporting electrolyte solution does not significantly affect the free energy of adsorption. This observation suggests that monolayer formation is best described in terms of the displacement of preadsorbed solvent molecules from the electrode surface rather than the removal of preadsorbed electrolyte ions.

Monolayers of this type represent useful model systems to address outstanding questions regarding how electrons and protons transfer through membranes. Control of how solution phase chemicals interact with these thin films, and what dictates their redox activity, are expected to impact our understanding of the mechanisms of biological reactions.

Acknowledgement

Funding from Forbairt, the Irish Science and Technology Agency, under Strategic Research Grant ST/98/414, is gratefully acknowledged.

References

1 A. Ulman, *An Introduction to Ultrathin Organic Films From Langmuir-Blodgett to Self-Assembly*, Academic Press, UK, 1991.
2 R. W. Murray, in *Molecular design of Electrode Surfaces*, ed. R. W. Murray, Wiley, New York, 1992, ch. 1.
3 M. D. Porter, T. B. Bright, D. L. Allara and C. E. D. Chidsey, *J. Am. Chem. Soc*., 1987, **109**, 3559.
4 C. E. D. Chidsey and D. N. Loiacono, *Langmuir*, 1990, **6**, 682.
5 R. V. Duevel and R. M. Corn, *Anal. Chem*., 1992, **64**, 337.
6 R. G. Nuzzo, L. H. Dubois and D. L. Allara, *J. Am. Chem. Soc*., 1990, **112**, 558.
7 J. M. Tour, L. Jones, D. L. Pearson, J. J. Lamba, T. P. Burgin, G. M. Whitesides, D. L. Allara, A. N. Parikh and S. V. Atre, *J. Am. Chem. Soc*., 1995, **117**, 9529.
8 R. J. Forster and J. P. O'Kelly, *J. Phys. Chem*., 1996, **100**, 3695.
9 A. J. Bard and L. R. Faulkner, *Electrochemical methods: Fundamentals and Applications*, Wiley, New York, 1980.
10 B. E. Conway, *Chem. Soc. Rev*., 1992, 253.
11 R. Parsons, *Chem. Rev*., 1990, **90**, 813.
12 R. L. Bretz and H. D. Abruña, *J. Electroanal. Chem*., 1995, **388**, 123.
13 R. J. Forster, *Analyst*, 1996, **121**, 733.
14 R. J. Forster, *Anal. Chem*., 1996, **68**, 3143.
15 R. De Levie, *Advances in Electrochemistry and Electrochemical Engineering*, Wiley, New York, 1986, vol. 13, p. 1.
16 C. A. Widrig, C. Chung and M. D. Porter, *J. Electroanal. Chem*., 1991, **310**, 335.
17 R. J. Forster, *Chem. Soc. Rev*., 1994, 289.
18 E. Laviron, *J. Electroanal. Chem*., 1974, **52**, 395.
19 P. Brown and F. C. Anson, *Anal. Chem*., 1977, **49**, 158.
20 P. He, R. M. Crooks and L. R. Faulkner, *J. Phys. Chem*., 1990, **94**, 1135.
21 R. J. Forster, *J. Electrochem. Soc*., 1997, **144**, 1165.
22 R. J. Forster, *Electrochemical Society Proceedings*, 1996, **96**, 65.
23 R. J. Forster, *Langmuir*, 1995, **11**, 2247.
24 J. Zhang and F. C. Anson, *J. Electroanal. Chem*., 1992, **331**, 945.
25 M. P. Soriaga, J. L. Stickney and A. T. Hubbard, *J. Electroanal. Chem*., 1983, **144**, 207.
26 M. P. Soriaga and A. T. Hubbard, *J. Am. Chem. Soc*., 1982, **104**, 3937.
27 M. P. Soriaga, J. H. White and A. T. Hubbard, *J. Phys. Chem*., 1983, **87**, 3048.
28 S. Trassatti, *J. Electroanal. Chem*., 1974, **53**, 335.
29 D. Acevedo, R. L. Bretz, J. D. Tirado and H. D. Abruña, *Langmuir*, 1994, **10**, 1300.
30 R. M. Wightman and D. O. Wipf, *Electroanalytical Chemistry*, ed. A. J. Bard, Marcel Dekker, New York, 1989, vol. 15.
31 C. P. Smith and H. S. White, *Anal. Chem*., 1992, **64**, 2398.
32 R. S. K. A. Gamage, A. J. McQuillan and B. M. Peake, *J. Chem. Soc., Faraday Trans*., 1991, **87**, 3653.
33 J. A. Dean, *Handbook of Organic Chemistry*, McGraw Hill, New York, 1987.
34 P. Delahay and I. Trachtenberg, *J. Am. Chem. Soc*., 1957, **79**, 2355.

Paper 8/03965H